

DESIGN OF A KINEMATIC SPINDLE FOR LOW-FORCE, LOW-SPEED APPLICATIONS

King-Fu Hii, Eric Wolsing, and R. Ryan Vallance

Precision Systems Laboratory, University of Kentucky, Lexington, KY *

Abstract

This paper describes a spindle for low-force, low-speed applications that is kinematically constrained and therefore based on the principles of exact constraint. The position and orientation of the spindle shaft is constrained at five contact points; four constraints are arranged radially around the shaft, and one constraint is located at the end of the shaft. In this paper, we describe the concept, detailed design of a prototype spindle, and analyses conducted during the detailed design. A simple 2D simulation is presented, which suggests that a shaft with a dominant periodic, multi-lobed roundness profile should cause the shaft's centerline to trace simple linear or circular trajectories. If the prototype spindle demonstrates repeatable error motions that are functions of the shaft rotation angle, then compensation may enable a spindle that is both highly repeatable and highly accurate. In addition, this spindle concept is amenable to micro positioning applications by incorporating position-controlled actuation at the constraint points. Although a prototype spindle was completed, experimental testing is not yet complete.

Keywords: machine design, spindle, kinematic constraint, exact constraint, axis of rotation

Introduction

In several ultra-high precision systems, linear motion is guided with sliding or rolling contact bearings that are arranged in a kinematic or exact constraint fashion [1]. A kinematic arrangement typically assures high repeatability, and accuracy is then attainable with accurate ways and rollers. In metrology applications, linear bearings employing thin polymer coatings have demonstrated that point contact between a bearing pad and way is sustainable with little wear [2]. The Nanostep profilometer from Rank Taylor Hobson (originally Nanosurf 2 [3]) and the NIST Molecular Measuring Machine [4] apply this technique. Despite the success of this approach in linear bearing systems, rotary bearings based on these principles have received little attention.

In the Precision Systems Laboratory at the University of Kentucky, we are designing an electro discharge micro milling machine [5]. The machine entails three axes of Cartesian motion and uses a pre-existing XY stage. Unlike a machine tool's spindle, a spindle in the micro EDM machine is not subjected to large forces, and high speeds are not necessary. Furthermore, there is an opportunity to simplify the machine configuration if the fine motion in the Z-axis is incorporated into the spindle. We are therefore interested in designing a high precision spindle for low-force and low-speeds that can eventually allow translation along the axis of the rotary motion.

In considering these requirements, we became interested in a spindle that used sliding contact constraints similar to those employed in linear bearings [2]. This paper describes the concept, design of a prototype spindle, and analyses conducted during the design. Results from a simple 2D simulation suggest that a shaft with a periodic, multi-lobed roundness profile should cause the shaft's centerline to trace simple linear or circular trajectories. A prototype spindle is fabricated, but measurement of error motions [6] is not complete and will therefore be presented in future work.

Conceptual Design of the Spindle

The kinematic spindle employs the principles of exact constraint [1] in establishing the position and orientation of a rotating shaft. Five constraints should be applied to the shaft so that the only free degree of freedom is rotation about the shaft's centerline. One approach to arranging the five constraints is to position a constraint acting axially along the centerline of the shaft and to position two pairs of constraints acting radially on the shaft. A finite distance along the shaft must separate the pair of radial constraints.

With appropriate nesting forces, the constraints can be established using five points of contact. This arrangement of constraints on a rotating shaft is illustrated in Fig 1. The axial constraint is simply a

* Precision Systems Laboratory, Mechanical Engineering, University of Kentucky, 210-A CRMS Building, Lexington, KY 40506. <http://www.engr.uky.edu/psl>.

rotating ball placed between the shaft's end and a rigid plate (magnetic base). The radial constraints are contact between the shaft and cylinders. Appropriate nesting forces are established by tension in the flexible drive belt and permanent magnets that lift the shaft towards the magnetic base. The shaft is free to rotate by sliding on the contact points when torque is transmitted from a servomotor through an o-ring belt. Radial and axial motions of the shaft are constrained by these five contact points. A similar configuration using line contact rather than point contact is used in a commercial μ EDM machine [7].

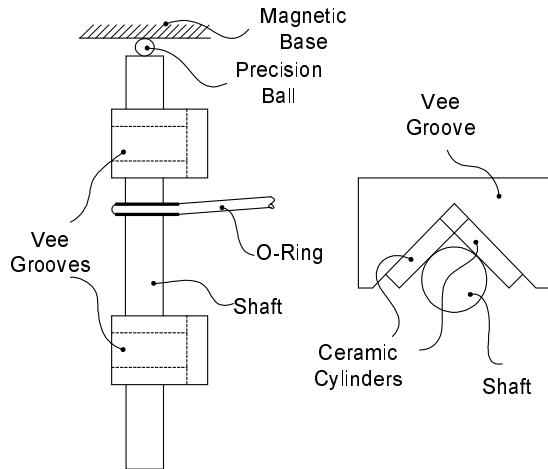


Fig 1: Kinematic Spindle Constrained with Five Contact Points

The principal advantage of the kinematic approach illustrated in Fig 1 is that repeatable error motions should be obtained. This means that radial and axial errors during shaft rotation should be repeatable functions of the shaft rotation angle. If repeatable motions are obtained, then compensation can provide further reduction in error motion. The disadvantage, however, is that sliding contact limits the rotational speed and loads that can be applied to the spindle shaft.

Detailed Design of a Prototype Spindle

To explore the repeatability of the shaft's error motions and the limits imposed by sliding contact, we designed and fabricated prototype spindles as illustrated in Fig 2. The 2 inch (50.8 mm) long shaft was machined from 1.5 inch (38.1 mm) diameter 440C stainless steel, case hardened to Rc 55-60 (Thomson 60 Case Shaft). A final grinding operation will be done in the Machine Dynamics Lab at Penn State to hopefully obtain roundness errors of about 10 micro inches (0.25 μ m).

An o-ring belt wraps around the shaft, and tension in the belt preloads the shaft against the radial

contact points. Axial preload is established by an array of permanent magnets mounted above the shaft in the top plate. We will investigate the spindle performance with sliding on ceramic rods and a thin layer of polymer (e.g. Nylon, UHMW, Delrin, etc). The contact surfaces are mounted into the vee-groove foundation and top plate. A 0.23 HP (175 W) brushless, slotless motor (Aerotech BMS60) and PWM amplifier drive the shaft. A 3:1 transmission is achieved with a 0.5 inch diameter pulley on the motor's shaft. The tension in the o-ring belt is adjustable by sliding the motor mount away from the spindle shaft.

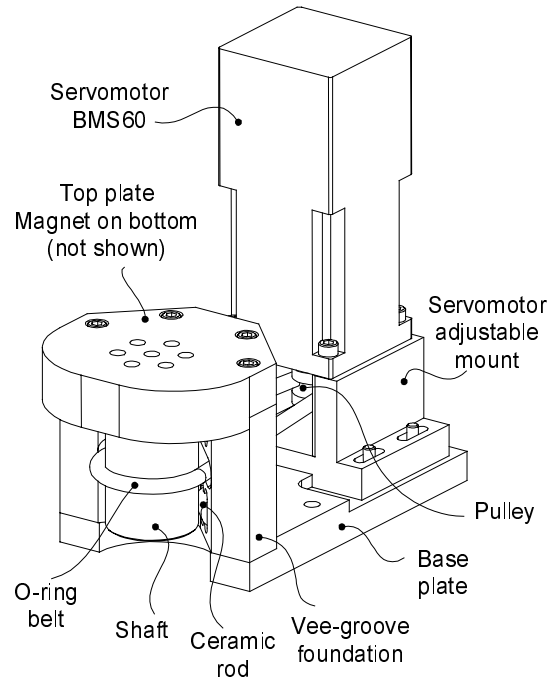


Fig 2: Prototype model for kinematic spindle

Analysis of the Detailed Design

The deterministic nature of exact constraint devices allows a thorough analysis during design. In analyzing the kinematic spindle, one should consider the following analyses:

1. Determine amount of tension required for transmitting power from motor to spindle shaft
2. Determine reaction and friction forces at five contact points based on belt tension and magnets
3. Analyze Hertzian contact
4. Size motor and transmission ratio

The tension in the o-ring belt can be determined using the Eq (1)-(3) where all values are in English units [8]. F_T is the tight-side tension, F_S is the slack-side tension, F_s is the minimum required tightening force, V is the belt velocity, θ is the wrap angle, μ is the coefficient of friction, F_c is centrifugal tension, A

is the belt cross section area, pwr is the power, and γ is the belt unit weight. The maximum tension necessary for the prototype spindle was estimated to be 3 lbs (13.6 N).

$$F_c = 0.104 \times 10^{-3} \gamma A V^2 \quad (1)$$

$$F_s = \frac{pwr}{2V} \frac{e^{\mu\theta} + 1}{e^{\mu\theta} - 1} + F_c \quad (2)$$

$$F_1 = F_s + \frac{pwr}{2V} \text{ and } F_0 = F_s - \frac{pwr}{2V} \quad (3)$$

A static analysis, which considers belt tension, magnetic preload, and dynamic friction forces, yields the components of the five reaction forces at the contact points.

Once the reaction forces are known, the Hertzian contact stresses can be determined and compared with material yield strength. A comprehensive contact analysis should include both the reactions that act normal to the contact surfaces and tangential forces due to friction. The designer should refer to comprehensive references on contact mechanics [9]. Since the centerline of the shaft is perpendicular to the centerline of the constraint rods, an elliptical contact region is expected.

2D Simulation of Shaft Error Motion

Unlike other spindles, the error motion of the kinematic spindle's shaft should be deterministic and predictable a priori. The principal source of error motion is the out-of-roundness in the shaft. We can therefore simulate the error motion of the shaft centerline for particular roundness profiles. The roundness of a shaft can be modeled with Eq (5) [10].

$$r(\theta_i) = R + \sum_{k=1}^{\infty} C_k \cos(k\theta_i - \Phi_k) \quad (4)$$

Where,

$$i = 1, 2, \dots, N \quad 0 \leq \theta_i \leq 2\pi$$

R = nominal shaft radius

C_k = amplitude of k-th harmonic

Φ_k = phase angle of a harmonic

A typical roundness profile for a ground shaft might have multiple lobes. In this paper, the shaft is assumed to have a dominant 2-lobe, 3-lobe, 4-lobe, or 5-lobe roundness profile. We expect that as the shaft rotates on the vee-grooves, the shaft's center will follow a path that depends upon the roundness profile of the shaft. Fig 3 shows an example of the error motion produced by a 2-lobed roundness profile for two particular angular positions of the shaft. The position of the shaft centerline will oscillate

horizontally (along the X' axis) as the 2 lobed shaft rotates counter clockwise.

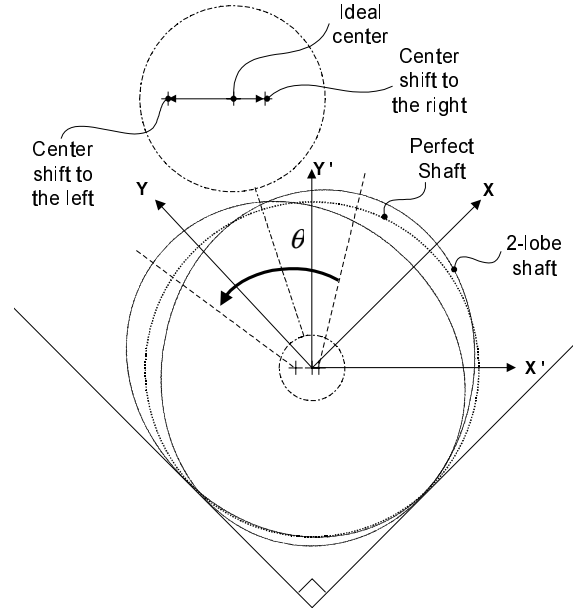


Fig 3: Displacement of Shaft Centerline for a Roundness Error with 2 Lobes

The shaft displacement error in the X and Y directions is given in Eq (6) and (7).

$$r_x(\theta_i) = \sum_{k=1}^{\infty} C_k \cos(k\theta_i - \Phi_k) \quad (5)$$

$$r_y(\theta_i) = \sum_{k=1}^{\infty} C_k \cos\left(k\left(\theta_i - \frac{\pi}{2}\right) - \Phi_k\right) \quad (6)$$

The magnitude of the shaft's displacement error at a particular shaft position is given in Eq (8).

$$r_{error}(\theta_i) = \left[\left(\sum_{k=1}^{\infty} C_k \cos(k\theta_i - \Phi_k) \right)^2 + \left(\sum_{k=1}^{\infty} C_k \cos\left(k\left(\theta_i - \frac{\pi}{2}\right) - \Phi_k\right) \right)^2 \right]^{1/2} \quad (7)$$

For the simulation, the amplitude of the dominant mode and groove angle were assumed to be 10 μm and 90°. Fig 4 illustrates the predicted trajectories of the shaft centerline for various quantities of lobes in the roundness profile. For shafts having (4n-2) lobes, the trajectory of the shaft's centerline should oscillate along the X' axis (Fig 3) with a peak displacement of 14.1 μm ($C_k/\cos(45^\circ)$). For shafts with 4n lobes, the trajectory of the shaft's center oscillates in and out of the groove, along the Y' axis (Fig 3) with maximum displacement of 14.1 μm . And, for shafts with 2n-1 lobes, the shaft's center should trace 2n-1 circles

around the ideal shaft center with a radius equal to the amplitude of the dominant harmonic mode (C_k).

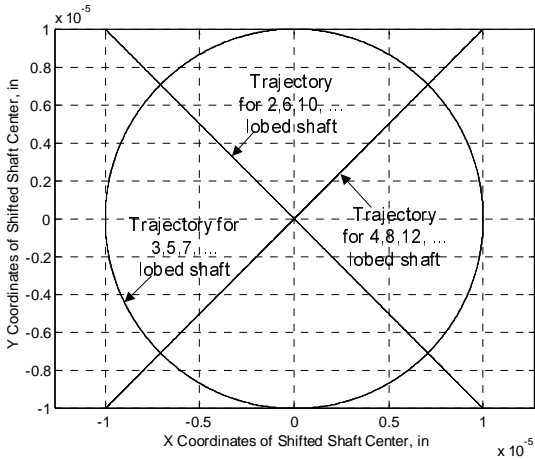


Fig 4: Trajectory of Shaft Centerline for Shafts with Various Quantities of Lobes

Fig 5 illustrates the magnitude of the shaft's displacement from the ideal center for a full rotation of the shaft for various quantities of lobes.

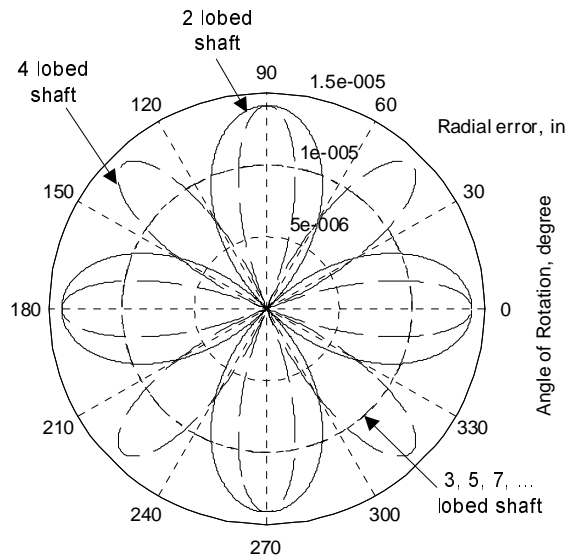


Fig 5: Magnitude of shaft displacement for any given angle of rotation for multi-lobed shafts

Conclusions and Future Work

Since sliding contact bearings with kinematic arrangement have been successful in ultra-high precision applications, we are now considering the performance of a spindle with sliding contact at kinematic constraints. This paper described the conceptual design and detailed design of a prototype spindle. A simple 2D simulation, suggests that shafts with multi-lobed roundness profiles should produce error motions with linear or circular trajectories of

the shaft centerline. Future experiments conducted on the prototype spindle will test this hypothesis and be used to study the wear due to sliding at the contact points. If repeatable error motions are observed experimentally, then future work will consist of passive and/or active compensation for attaining a precise and accurate axis of rotation.

References

- [1] Blanding, D.L. *Exact Constraint: Machine Design Using Kinematics Principles*. ASME Press. New York. 1999.
- [2] Smith, S.T., H. Yang, and R.M. Seugling. "Polymeric Bearings for Nanotechnology Applications". *Proceedings of the American Society for Precision Engineering Summer Topical Meeting on Precision Bearings and Spindles*. State College, PA. June 18-19, 2001. p. 70-75.
- [3] Lindsey, K., S.T. Smith, and C.J. Robbie. "Sub-Nanometer Surface Texture and Profile Measurement with 'Nanosurf 2'". *Annals of the CIRP*. Vol. 37. p. 519-522.
- [4] Evans, C.R., R.S. Polvani, F.E. Scire, A.W. Ruff, X.Z. Hu, and E.C. Teague. "Way Systems for the Molecular Measuring Machine". 5th Int. Precision Engineering Seminar. Sept. 18-22, 1989. Monteyrey, CA.
- [5] Hii, K.F., X. Zhao, and R.R. Vallance. "Design of a Precision Electro Discharge Micro Milling Machine". *Proceedings of the American Society of Precision Engineers Annual Conference*. Scottsdale, Arizona. October 22-27, 2000. p. 353-356.
- [6] "Axes of Rotation – Methods for Specifying and Testing". ASME 89.3.4-1985. American Society of Manufacturing Engineers. 1985.
- [7] Masaki, T., T. Mizutani, K. Yonemauchi, and A. Tanaka. "Electric Discharge Machining Method and Apparatus for Machining a Microshaft". U.S. Patent #4,900,890. Issued Feb. 13, 1990.
- [8] Burr, A. H. and Cheatham, J. B. *Mechanical Analysis And Design*. 2nd Edition. Prentice Hall. Englewood Cliffs, New Jersey. 1995.
- [9] Johnson, K.L. *Contact Mechanics*. Cambridge University Press. Cambridge, Great Britain. 1987.
- [10] Cho, N. and J. Tu. "Roundness modeling of machined parts for tolerance analysis". *Precision Engineering*. 25 (2001). p. 35-47.